Estimates in (*1*) indicate that meteorites >500 g accumulated during the Early Ordovician at a rate two orders of magnitude higher than today. The discrepancy between this estimate and the order of magnitude enhancement for extraterrestrial dust accretion may be related to the greater statistical uncertainty for the meteorite flux calculations. The Ordovician meteorite flux represents an average for 1.17 My, whereas accretion rates based on recent meteorite distributions in desert areas represent only the past ~0.05 My (*18*). If meteorite influx to Earth is episodic, this would be an important circumstance to consider. Alternatively, the discrepancy could be related to differences in the dynamic behavior of the different source regions for meteorites and extraterrestrial dust. Meteoroids are products of parent body fragmentation in the asteroid belt, whereas extraterrestrial dust is derived from asteroidal as well as cometary (the Kuiper belt, the Oort cloud) and interstellar sources.

We do not know to what extent the ~1.75-My period we studied represents an anomaly in terms of extraterrestrial matter influx, or whether it is representative of a much longer time interval. However, it is likely that the abundant meteorites reflect a short event such as a catastrophic breakup of a meteorite parent body in the asteroid belt. Analyses of chromite grains from the Österplana Ark 001 meteorite indicate that it is an H or L chondrite (*5*). Studies of recent meteorites have revealed a high abundance of heavily shocked and degassed L chondrites with Ar-Ar ages around 500 Ma, suggesting a major impact on the L chondrite parent body at this time (*19*). It is possible that the high meteorite density on the Early Ordovician sea floor is somehow related to the disruption of the L chondrite parent body at ~500 Ma. If this is correct, the early Paleozoic limestone record may contain important further information about the timing, causes, and effects of this major event in the history of the solar system.

Table 3. Results of $^{87}Sr/^{86}Sr$ isotopic analyses of biogenic calcite. The first two samples are unidentified shells; the third sample at +3.5 m is a trilobite pygidium. All values are normalized to a value of 0.710140 for NBS 987 standard. Errors are 2σ of the mean of repeated measurements. Depth is relative to the base of the gray interval (Fig. 1).

Depth (m)	$^{87}Sr/^{86}Sr$
−3.9	0.708858 ± 12
+0.9	0.708792 ± 11
+3.5	0.708820 ± 12

REFERENCES AND NOTES

1. B. Schmitz, M. Lindström, F. Asaro, M. Tassinari, *Earth Planet. Sci. Lett.* **145**, 31 (1996).
2. Os isotope analyses were as described [E. H. Hauri and S. R. Hart, *ibid.* **114**, 353 (1993)] (*8*). Os was extracted from the samples by means of a NiS fire assay, followed by distillation and a single ion-exchange resin bead clean-up step. Isotopic measurements were done by negative thermal ionization mass spectrometry at WHOI using the single-collector NIMA-B. Os data were blank-corrected using an average total procedural blank of 1.55 pg of Os per gram of fusion reagent, with a mean $^{187}Os/^{186}Os$ ratio of 2.571. Re was measured on different sample splits by isotope dilution inductively coupled plasma–mass spectrometry at MIT. Typical uncertainties for Re concentrations are <5%.
3. Element results were obtained by instrumental neutron activation analysis (INAA) at ACTLABS, Ontario [see (*1*)]. $^{87}Sr/^{86}Sr$ ratios were determined with a Finnigan MAT 261 mass spectrometer as described (B. Schmitz, S. L. Ingram, D. T. Dockery, G. Åberg, *Chem. Geol. Isotope Geosci.*, in press).
4. P. Thorslund, F. E. Wickman, J. O. Nyström, *Lithos* **17**, 87 (1984).
5. J. O. Nyström, M. Lindström, F. E. Wickman, *Nature* **336**, 572 (1988).
6. P. Jenniskens *et al.*, *Meteoritics* **29**, 246 (1994).
7. B. K. Esser and K. K. Turekian, *Geochim. Cosmochim. Acta* **52**, 1383 (1988).
8. B. Peucker-Ehrenbrink, G. Ravizza, A. W. Hofmann, *Earth Planet. Sci. Lett.* **130**, 155 (1995).
9. W. H. Burke *et al.*, *Geology* **10**, 516 (1982).
10. R. A. F. Grieve, *Annu. Rev. Earth Planet. Sci.* **15**, 245 (1987); ———, J. Rupert, J. Smith, A. M. Therriault, *GSA Today* **5**, 189 (1995); M. J. Benton, *Science* **268**, 52 (1995).
11. M. Lindström, *Geol. Rundsch.* **60**, 419 (1971); R. B. Pedersen, D. L. Bruton, H. Furnes, *Terra Nova* **4**, 217 (1992).
12. B. K. Esser and K. K. Turekian, *Geochim. Cosmochim. Acta* **57**, 3093 (1993).
13. K. H. Wedepohl, *ibid.* **59**, 1217 (1995).
14. G. Ravizza and K. K. Turekian, *ibid.* **53**, 3257 (1989).
15. An estimate for the diffusive Ir loss based on an Ir profile across the Österplana Ark 009 meteorite and the limestone surrounding Österplana Ark 001 (*1*) indicates that ~50% of the Ir was lost from the meteorites by diffusion. However, ~25% of this mobile Ir was redeposited within 10 cm of the meteorite.
16. G. Ravizza and G. M. McMurtry, *Geochim. Cosmochim. Acta* **57**, 4301 (1993).
17. B. Peucker-Ehrenbrink, *ibid.* **60**, 3187 (1996).
18. P. A. Bland, F. J. Berry, T. B. Smith, S. J. Skinner, C. T. Pillinger, *ibid.*, p. 2053.
19. H. Haack, P. Farinella, E. R. D. Scott, K. Keil, *Icarus* **119**, 182 (1996); D. D. Bogard, D. H. Garrison, M. Norman, E. R. D. Scott, K. Keil, *Geochim. Cosmochim. Acta* **59**, 1383 (1995).
20. M. Lindner, D. A. Leich, G. P. Russ, J. M. Bazan, R. J. Borg, *Geochim. Cosmochim. Acta* **53**, 1597 (1989).

21. We thank G., S., and S. Thor for finding the meteorites, G. Ravizza for Re analyses, S. Hart for the use of the clean-lab and NIMA-B, G. Åberg for Sr isotope analyses, and B. K. Esser and an anonymous referee for valuable comments. Supported by the Bank of Sweden Tercentenary Foundation, the E. and V. Hasselblad Foundation, and Byggordning Konsult AB (B.S.), and by the J. B. Cox Endowed Fund, the Penzance Fund, and the NSF (B.P.-E.). This is WHOI contribution 9538.

12 June 1997; accepted 25 August 1997

Measurements of $^{12}C/^{13}C$, $^{14}N/^{15}N$, and $^{32}S/^{34}S$ Ratios in Comet Hale-Bopp (C/1995 O1)

David C. Jewitt,* Henry E. Matthews, Tobias Owen, Roland Meier

The $^{12}C/^{13}C$, $^{14}N/^{15}N$, and $^{32}S/^{34}S$ isotope ratios in comet Hale-Bopp (C/1995 O1) were determined through observations taken with the James Clerk Maxwell Telescope. Measurements of rare isotopes in HCN and CS revealed isotope ratios of $H^{12}CN/H^{13}CN = 111 \pm 12$, $HC^{14}N/HC^{15}N = 323 \pm 46$, and $C^{32}S/C^{34}S = 27 \pm 3$. Within the measurement uncertainties, the isotopic ratios are consistent with solar system values. The cometary volatiles thus have an origin in the solar system and show no evidence for an interstellar component.

The isotopic abundances of abundant elements (C, N, O, S, and others) may reveal where cometary material originated. In the current paradigm, cometary matter was captured from the solar nebula at the time of the formation of the planetary system and should preserve a record of isotopic abundance ratios in the nebula 4.5×10^9 years old (*1*). Isotopic anomalies in comets, if they exist, might reveal patterns of pollution of the solar nebula by nearby supernovae, or gas phase reactions in the pre-planetary disk, or even the existence of interstellar comets.

Nearly-solar isotope ratios were measured by spacecraft passing through the coma of P/Halley (*2*, *3*). The $^{12}C/^{13}C$ ratio has been determined in a few other comets from ground-based data [Ikeya 1963a (*4*), Kohoutek 1973f (*5*), and Kobayashi-Berger-Milon 1975IX (*6*)], and the ratio is consistent with a solar system origin for all. Many of these measurements relied on high-reso-

D. C. Jewitt, T. Owen, R. Meier, Institute for Astronomy, University of Hawaii, 2680 Woodlawn Drive, Honolulu, HI 96822, USA.
H. E. Matthews, Herzberg Institute of Astrophysics, National Research Council, 5071 West Saanich Road, Victoria, BC V8X 4M6, Canada and Joint Astronomy Centre, 660 North A'ohoku Place, Hilo, HI 96720–6030, USA.
*Visiting astronomer at the James Clerk Maxwell Telescope, which is operated by The Joint Astronomy Centre on behalf of the Particle Physics and Astronomy Research Council of the United Kingdom, the Netherlands Organisation for Scientific Research, and the National Research Council of Canada.

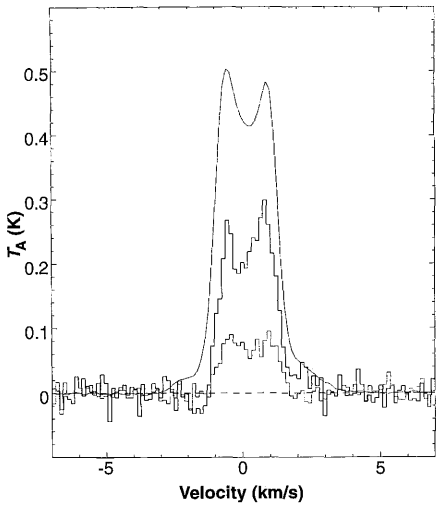

Fig. 1. Spectra of $H^{12}CN(4-3)$ at 354.5055 GHz (top curve), $H^{13}CN(4-3)$ at 345.3398 GHz (middle curve), and $HC^{15}N(4-3)$ at 344.2003 GHz (bottom curve) obtained with receiver B3 on 16.71 February 1997 UT. The $H^{12}CN$ line has been scaled down by a factor of 30 for easy comparison.

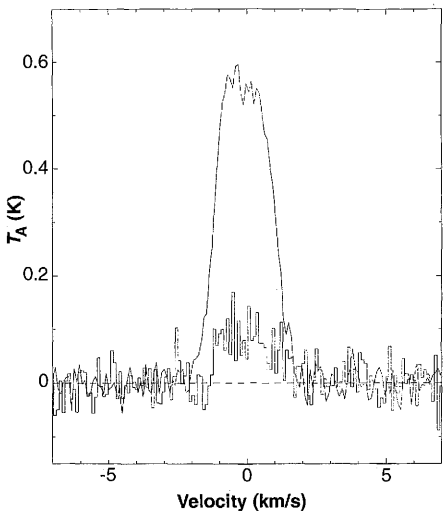

Fig. 2. Spectra of $C^{32}S(5-4)$ at 244.9356 GHz (top curve) and $C^{34}S(5-4)$ at 241.0162 GHz (bottom curve) obtained with receiver A2 on 24.02 February 1997 UT. The $C^{32}S$ line has been scaled down by a factor of 5 for easy comparison.

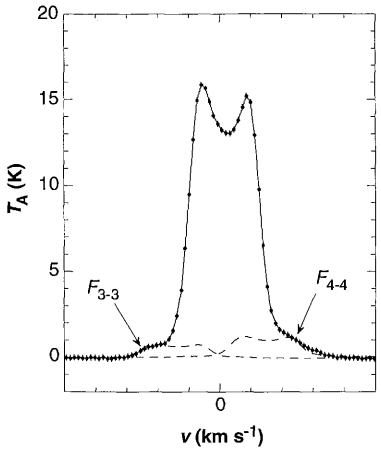

Fig. 3. The HCN(4-3) line observed at 16.71 February 1997 UT. Error bars denote statistical uncertainties estimated from the noise in the data. Systematic errors due to fitting and subtraction of a polynomial spectral baseline are present but not shown. The hyperfine components are indicated, together with fits.

lution ($\lambda/\Delta\lambda \approx 10^5$) optical spectroscopy of the CN and Swan bands of C_2. Their accuracy depended critically on the removal of line and continuum contamination from the spectra. Spectral resolutions in the submillimeter-wavelength regime now routinely exceed 10^6, minimizing errors caused by line blending and continuum contamination. Accordingly, we took advantage of the appearance of Hale-Bopp and a period of unusually good daytime atmospheric conditions to measure isotope ratios from rotational lines at submillimeter wavelengths. This report supersedes our preliminary announcement of the isotope measurements (*7*).

Observations were taken with the 15-m-diameter James Clerk Maxwell Telescope (JCMT) located at an altitude of 4 km near the summit of Mauna Kea, Hawaii (*8*). The pointing of the telescope was updated from the comet ephemeris in real-time with the use of a linear interpolation algorithm. The accuracy of the telescope pointing was measured by repeated observations of known galactic and extragalactic continuum sources near Hale-Bopp. On 16 and 24 February 1997 universal time (UT), the zenith optical depth at 225 GHz was in the range $0.03 \leq \tau_{225} \leq 0.05$, corresponding to precipitable water columns of 0.5 to 1.0 mm. Additional measurements were obtained on 22 March 1997 UT under less favorable conditions, with $\tau_{225} = 0.15$ (3.5 mm H_2O). The geometric parameters of the observations are listed in Table 1.

Two different receivers were used for the 350-GHz (B3) and 240-GHz (A2) spectral windows. Isotopomers of HCN were observed with the B3 spectral line receiver, frequency-switched by ±8.1 MHz once every 30 s to provide sky cancellation (Fig. 1). Channel spacing with B3 was 156 kHz, corresponding to a spectral resolution $\lambda/\Delta\lambda = 1.9 \times 10^6$ and to velocity resolution $\Delta V = 0.15$ km s^{-1}. The effective beam diameter was 13.3 ± 0.2 arc sec half-power beam width (HPBW). Cometary CS was observed with receiver A2, beam-switched by 180 arc sec in azimuth at 1 Hz (Fig. 2). Channel spacing with A2 was 78 kHz, corresponding to $\lambda/\Delta\lambda = 2.6 \times 10^6$ ($\Delta V = 0.12$ km s^{-1}). The effective beam diameter was 19.7 ± 0.5 arc sec HPBW. These small beam measurements refer to the inner few-thousand kilometers of the coma, where collisional excitation rates dominate fluorescence (*9*).

Measurements of the line areas in the Hale-Bopp spectra, measured ±3 km s^{-1} from line center, are given in Table 2. Uncertainties in the areas of the bright HCN and CS lines were estimated from repeated measurements and resulted primarily from pointing errors in the JCMT. We minimized the effects of possible temporal variability in the outgassing of the comet by observing the abundant and rare isotopomers close together in time. Monitoring of the HCN line showed variations on time scales of hours that were about ±10%, scarcely larger than uncertainties due to atmospheric instability and telescope pointing errors. The uncertainties in the areas of fainter lines are dominated by sky noise and by uncertainties in the polynomial baseline subtraction. However, the primary source of uncertainty in the measured isotope ratios of C and N is in the correction for opacity in the bright lines of the most abundant isotopomer. Asymmetries in the spectral lines show that the outflow is anisotropic, so that spherically symmetric radiative transfer models cannot be applied. Instead, we used an empirical method to assess the beam-averaged optical depth in the coma.

The HCN(4-3) line consists of six hyperfine components, two of which are resolved as broad wings to the line in our data (Fig. 3). The hyperfine quantum level F = 3-3 and F = 4-4 components are separated from the F = 4-3 line by 1.977 MHz (−1.67 km s^{-1}) and −1.610 MHz (1.36 km s^{-1}), respectively, and each carries 2.17% of the line flux (*10*). The F = 3-3 component is distinct from the line core in our spectra

Table 1. Geometric parameters of Hale-Bopp on the dates of observation. R, heliocentric distance; Δ, geocentric distance; α, phase angle; ε, elongation; and S, linear scale in the plane of the sky.

UT date (1997 UT)	R (AU)	Δ (AU)	α (degrees)	ε (degrees)	S (km/arc sec)
16 February	1.20	1.71	−34.3	43.0	1240
24 February	1.11	1.57	−38.9	44.9	1140
22 March	0.93	1.32	+49.1	44.7	960
19 July	2.00	2.79	−15.5	31.8	2037

and provides a measure of the line core optical depth. For the 16 February 1997 data, we fit the F = 3-3 component and with it obtained a line area ratio $F_{3\text{-}3}/F_{core}$ = 0.029 ± 0.003. This is larger than the theoretical (local thermodynamic equilibrium) value $F_{3\text{-}3}/F_{core}$ = 0.0217 and consistent with depression of the line core intensity by a factor f = (0.029 ± 0.003)/0.0217 = 1.34 ± 0.14. Using the same model, we independently fit the F = 4-4 component and obtained $F_{4\text{-}4}/F_{core}$ = 0.032 ± 0.004 and f = 1.47 ± 0.18. The weighted means from the $F_{3\text{-}3}$ and $F_{4\text{-}4}$ ratios are 0.031 ± 0.002, and f = 1.43 ± 0.11. The good agreement between $F_{3\text{-}3}$ and $F_{4\text{-}4}$ in Hale-Bopp suggests that hyperfine anomalies such as those reported in the interstellar medium (ISM) (*11*) and in Halley (*12*) are not present in Hale-Bopp, at least on the dates of observation. On 22 March, we determined a larger core depression factor, consistent with the increase in the outgassing from the nucleus during February and March. Apparent and corrected line area ratios are summarized in Table 3.

The accuracy of the fits to the hyperfine components of HCN is dependent on the accuracy of subtraction of the continuum adjacent to the emission line. An independent test of the hyperfine method was obtained on 19 July 1997 by measurement of $H^{12}CN/H^{13}CN$ in Hale-Bopp at 2 astronomical units (AU) heliocentric distance (Table 3). At this larger distance the effects of optical depth are reduced by an order of magnitude, and the line area ratio should approach the true isotopic ratio. The apparent line area ratio on 19 July (102 ± 12) is indeed close to the corrected ratio deduced from data taken in February (100 ± 12) and March (130 ± 12) and is quite different from the line area ratio (≈65) measured in the earlier months.

We find a mean $H^{12}CN/H^{13}CN$ = 111 ± 12 from measurements at all three epochs in Table 3, where the uncertainty reflects systematic rather than random errors. Lis *et al.* (*13*) independently obtained $H^{12}CN/H^{13}CN$ = 90 ± 15 which, within the uncertainties, is consistent with our determination. Previous measurements of $^{12}C/^{13}C$ in comets cluster near the solar system value of 89 (Fig. 4) (*14*), but with differences that have sometimes been thought significant (*1*, *15*, *16*). Our ratio is larger than the nominal solar system value, but the difference is not statistically significant, whereas the local ISM has $^{12}C/^{13}C$ = 77 ± 7 (*17*), which is statistically different from the Hale-Bopp ratio. Likewise, the Hale-Bopp ratio $HC^{14}N/HC^{15}N$ = 323 ± 46 is slightly larger than, but formally consistent with, the solar system ratio of $^{14}N/^{15}N$ = 270 (*14*). It is also consistent within errors with the local ISM, which has $^{14}N/^{15}N \approx 460 \pm 100$ (*18*). The isotopic ratios in N have not been previously measured in comets, although a 3σ limit $C^{14}N/C^{15}N > 270$ was determined in Halley (*16*).

The $C^{32}S$ line has a peak antenna temperature T_A of only 3 K and is taken to be optically thin. Consequently, we have made no correction for opacity, and the line area ratio is equal to the isotopic abundance ratio. We measured $C^{32}S/C^{34}S$ = 27 ± 3, with the uncertainty reflecting the faintness of the $C^{34}S$ line. The measured ratio is compatible, within the errors, with the solar system value of 22.6 (*14*), with the in situ determination of the ionic ratio $^{32}S^+/^{34}S^+ = 22^{+6}_{-4}$ in Halley (*19*), and with the local ISM ratio of $^{32}S/^{34}S$ = 32 ± 5 (*20*).

The solar system and cometary isotopic ratios are compared in Fig. 4. Although the C, N, and S isotope ratios all fall slightly above the corresponding solar system values, the differences are statistically insignificant. In this regard, the ratio $(^{12}C/^{13}C) \times (^{15}N/^{14}N)$ is independent of optical depth corrections. The terrestrial (0.33) and cometary values (0.34 ± 0.06) of this ratio are indistinguishable. Thus, we feel that Fig. 4 provides no evidence that cometary isotopic ratios differ from canonical solar system ones. Furthermore, the $(^{12}C/^{13}C) \times (^{15}N/^{14}N)$ ratio in the ISM varies (with considerable scatter) from <0.03 at the galactic center to 0.17 in the solar neighborhood (*17*). These differences in isotopic abundances are understood in terms of models for galactic evolution (*17*, *21*). Thus, the C and N isotopic ratios eliminate the possibility that Hale-Bopp had an interstellar origin

Table 2. Measurements of rotational lines. ν, line frequency; Date, midpoint of each observation; τ_{225}, zenith optical depth at 225 GHz measured with the Caltech Submillimeter Observatory radiometer adjacent to the JCMT. The line area was determined within a ±3 km/s–wide window centered on each emission line.

Species	ν (GHz)	Date (1997 UT)	τ_{225}	Line area (K km s^{-1})
$H^{12}CN$(4-3)	354.5055	16.72 February	0.03–0.05	38.5 ± 0.7
		22.75 March	0.15	75.9 ± 1.5
		19.87 July	0.05	5.9 ± 0.2
$H^{13}CN$(4-3)	345.3398	16.35 February	0.03–0.05	0.55 ± 0.05
		22.82 March	0.15	1.2 ± 0.1
		19.88 July	0.05	0.058 ± 0.008
$HC^{15}N$(4-3)	344.2003	16.44 February	0.03–0.05	0.17 ± 0.02
$C^{32}S$(5-4)	244.9356	23.93 February	0.09	6.67 ± 0.1
$C^{34}S$(5-4)	241.0162	24.02 February	0.09	0.25 ± 0.03

Table 3. Isotope ratios derived from the spectrum lines. LAR, line area ratio determined from the data in Table 2; f, correction for depression of the brighter isotopomer determined from the hyperfine components as described in the text. The isotope ratios for Hale-Bopp, the solar system, and the interstellar medium are indicated by comet, sun, and ISM, respectively.

Ratio	Date (1997 UT)	LAR	f	Comet	Sun	ISM
$H^{12}CN/H^{13}CN$	16 February	70 ± 6	1.43 ± 0.11	100 ± 12	89.9	77 ± 7
$H^{12}CN/H^{13}CN$	22 March	64 ± 5	2.05 ± 0.05	130 ± 12	89.9	77 ± 7
$H^{12}CN/H^{13}CN$	19 July	102 ± 12	1.00	102 ± 12	89.9	77 ± 7
Mean		–	–	111 ± 12	89.9	77 ± 7
$HC^{14}N/HC^{15}N$	16 February	226 ± 27	1.43 ± 0.11	323 ± 46	272.2	450 ± 100
$C^{32}S/C^{34}S$	24 February	27 ± 3	1.00	27 ± 3	22.6	32 ± 5

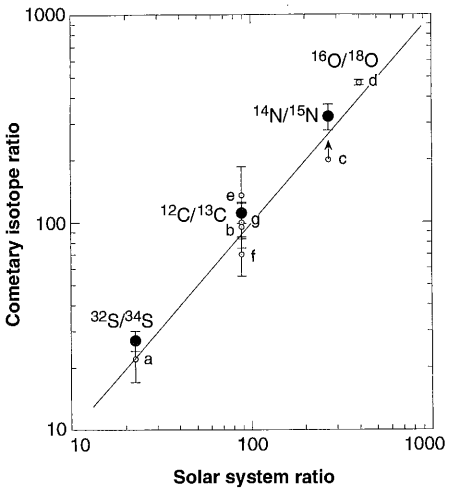

Fig. 4. Comparison of isotope ratios measured in Hale-Bopp (●) with those measured elsewhere (⊙) in the solar system (*14*). Earlier isotope ratio determinations are shown in Halley (points a to d) (*3*, *16*, *19*), in Kohoutek 1973f (point e) (*5*), in Ikeya 1963a (point f) (*4*), and in Kobayashi-Berger-Milon 1975IX (point g) (*6*).

and are consistent with prevailing theories for the origin of comets in the outer regions of the sun's pre-planetary accretion disk.

REFERENCES AND NOTES

1. V. Vanysek, in *Comets in the Post-Halley Era*, R. L. Newburn *et al.*, Eds. (Kluwer, Dordrecht, Netherlands, 1991), pp. 879–895.
2. E. K. Jessberger and J. Kissel, in (*1*), pp. 1075–1092.
3. P. Eberhardt, M. Reber, D. Krankowsky, R. Hodges, *Astron. Astrophys.* **302**, 301 (1995).
4. A. Stawikowski and J. Greenstein, *Astrophys. J.* **140**, 1280 (1964).
5. A. Danks, D. Lambert, C. Arpigny, *ibid.* **194**, 745 (1974).
6. V. Vanysek, in *Comets, Asteroids and Meteorites*, A. H. Delsemme, Ed. (Univ. of Toledo Press, Toledo, OH, 1977), p. 499.
7. H. E. Matthews and D. C. Jewitt, *IAU Circular 6567* (1997).
8. Most of the observations were carried out in daytime. The JCMT dish is protected from direct solar heating and from wind buffeting by a Goretex membrane that is transparent to submillimeter wavelengths. Mechanical stability of the JCMT allows pointing to about ±1.5 arc sec root mean square over much of the sky.
9. D. Bockelee-Morvan *et al.*, *Astron. Astrophys.* **141**, 411 (1984).
10. D. Bockelee-Morvan, R. Padman, J. K. Davies, J. Crovisier, *Planet. Space Sci.* **42**, 655 (1994).
11. Y. X. Cao, Q. Zeng, S. Deguchi, O. Kameya, N. Kaifu, *Astron. J.* **105**, 1027 (1993).
12. F. Schloerb, M. J. Claussen, L. Tacconi-Garman, *Astron. Astrophys.* **187**, 469 (1987).
13. D. Lis *et al.*, *IAU Circular 6566* (1997).
14. E. Anders and N. Grevesse, *Geochim. Cosmochim. Acta* **53**, 197 (1989).
15. S. Wyckoff *et al.*, *Astrophys. J.* **339**, 488. (1989).
16. M. Kleine, S. Wyckoff, P. Wehinger, B. A. Peterson, *ibid.* **439**, 1021 (1995).
17. T. L. Wilson and R. J. Rood, *Annu. Rev. Astron. Astrophys.* **32**, 191 (1994).
18. G. Dahmen, T. Wilson, F. Matteucci, *Astron. Astrophys.* **295**, 194 (1995).
19. D. Krankowsky *et al.*, *Nature* **321**, 326. (1986).
20. Y.-N. Chin, C. Henkel, J. B. Whiteoak, N. Langer, E. B. Churchwell, *Astron. Astrophys.* **305**, 960 (1996).
21. M. Frerking, R. W. Wilson, R. A. Liuke, P. G. Wannier, *Astrophys. J.* **240**, 65. (1980).

22. We thank the operators of JCMT for their assistance, and B. Marsden and D. Tholen for help with the ephemerides. Supported by a grant from NASA Planetary Astronomy Program to D.C.J.

7 May 1997; accepted 12 August 1997

Midwinter Start to Antarctic Ozone Depletion: Evidence from Observations and Models

H. K. Roscoe,* A. E. Jones, A. M. Lee

Measurements of total ozone at Faraday, Antarctica (65°S), by a visible spectrometer show a winter maximum. This new observation is consistent with the descent of air within the polar vortex during early winter, together with ozone depletion starting in midwinter. Chemical depletion at these latitudes in midwinter is suggested by existing satellite observations of enhanced chlorine monoxide and reduced ozone above 100 hectapascals and by reduced ozone in sonde profiles. New three-dimensional model calculations for 1994 confirm that chemical ozone depletion started in June at the sunlit vortex edge and became substantial by late July. This would not have been observed by most previous techniques, which either could not operate in winter or were closer to the Pole.

Dramatic ozone depletion was first reported at a high-latitude Antarctic site (76°S), where it was observed to start in late August (*1*). This is the time in the spring when the stratosphere becomes sunlit at this latitude, whereby the photochemistry leading to ozone depletion is initiated. Most subsequent investigations of the ozone hole also concentrated on sites at these high latitudes. There were few investigations at sites further north, because dynamical activity near the edge of the Antarctic vortex made it more difficult to see the depletion. Hence, the ozone hole has usually been considered to occur exclusively during the spring and often is perceived to be associated with the time of year rather than with the availability of sunlight at that location. The possibility that depletion might occur during winter within the vortex equatorward of 67°S, where there is always enough sunlight to initiate photochemistry, had not been subjected to a conclusive test.

Observations of total ozone during the Antarctic winter are sparse. Reliable observations by a Dobson spectrophotometer cannot be made poleward of 60°S in midwinter (*2*) because the Dobson observes ultraviolet (UV) light. The satellite-borne Total Ozone Mapping Spectrometer (TOMS) cannot make accurate observations in June or July at 65°S (*3*) because it also observes solar UV. The satellite-borne Tiros Operational Vertical Sounder (TOVS) has poor accuracy over the central Antarctic plateau in winter and reduced accuracy at the edge of Antarctica (*4*). The satellite-borne Microwave Limb Sounder (MLS) can only measure the column of ozone above 100 hPa, only measures south of 40°S for alternate 36-day periods, and was not launched until 1991 (*5*).

Ozone absorbs visible light, as well as the UV light observed by the Dobson. Observations by a visible spectrometer of light scattered from the zenith sky can be made to 91° solar zenith angle (SZA), that is, throughout the winter at 65°S. In 1990, a ground-based visible spectrometer of the design Système d'Analyse par Observations Zénithales [SAOZ (*6*)] was installed at Faraday (65.3°S, 65.3°W). SAOZ records spectra throughout the day, deducing ozone from absorption between 500 and 560 nm at SZAs between 87° and 91°.

The ability to discern trends in ozone on any time scale is determined by the stability of the measurement calibration. In previous work (*7*), we examined the stability of measurements of ozone by SAOZ at Faraday and have now improved it (*8*). The stability of the zero of the measurement is now equivalent to an annual cycle of less than 25 Dobson units (DU) and to a change during winter of less than 10 DU. Hence the measurements by SAOZ at Faraday are the first reliable operational measurements of total ozone throughout the winter at the sunlit edge of the vortex. Although a SAOZ was installed at Dumont d'Urville in 1988 (*6*), at 140°E the vortex is more often displaced away from that site's side of Antarctica.

We analyzed daily total ozone values in winter for the years 1990, 1991, and 1994 (Fig. 1). Values from 1992 and 1993 were excluded, because air-mass factors (AMFs) of visible light are particularly sensitive to the profile of aerosol in the stratosphere when amounts are large, and the eruption of Mount Pinatubo greatly enhanced aerosol amount and variability in Antarctica for the 2 years from November 1991. This variability makes it difficult to calculate reliable AMFs until 1994, when the amount of aerosol was smaller and less variable (*9*). A winter maximum in ozone is discernible in all three winters (Fig. 1), especially in the more heavily smoothed lower curves, where the size of the maximum within the winter period is much larger than 10 DU in 1990 and 1991.

The question follows, what is the cause of the observed maximum? There are various mechanisms that might cause an increase in ozone: (i) a decrease in tropopause height, associated with short time-scale synoptic weather systems (*10*); (ii) the vortex edge moving from one side of Faraday to the other, which certainly results in increased total ozone in the spring over the course of several days, as shown in the large short time-scale fluctuation in Fig. 2 at the end of

H. K. Roscoe and A. E. Jones, British Antarctic Survey, Natural Environment Research Council, High Cross, Madingley Road, Cambridge CB3 0ET, UK.
A. M. Lee, Centre for Atmospheric Science, Department of Chemistry, University of Cambridge, Lensfield Road, Cambridge, CB2 1EW UK.

*To whom correspondence should be addressed at h.roscoe@bas.ac.uk